Article type : Research Article

Synergistic interaction of N-3-Br-Benzyl-noscapine and docetaxel abrogates oncogenic potential of breast cancer cells

Running title: Synergistic effect of N-3-Br-Benzyl-noscapine and docetaxel

Shruti Gamya Dash[1], Srinivas Kantevari[2], Swaroop Kumar Pandey[3,4] and Pradeep Kumar Naik[1*]

[1]Centre of Excellence in Natural Products and Therapeutics, Department of Biotechnology and Bioinformatics, Sambalpur University, Jyoti Vihar, Burla, Sambalpur-768 019, Odisha, India

[2]Fluoro and agrochemicals Division, CSIR-Indian Institute of Chemical Technology, Hyderabad 500 007, India

[3]Bencos Research Solutions, New Link Road, Andheri West, Mumbai-400053, Maharashtra, India.

[4]Present address: Department of Life Sciences and the National Institute for Biotechnology in the Negev, Ben-Gurion University of the Negev, Beer-Sheva, 84105, Israel.

***For correspondence:** Phone No.: +91-9479268802; E-mail: pknaik1973@gmail.com

ABSTRACT

Noscapine, an opium alkaloid was discovered to bind tubulin, arrest dividing cells at mitosis, and selectively induced apoptosis to cancer cells. One of its derivatives, N-3-Br-Benzyl-Noscapine (Br-Bn-Nos) was demonstrated to have improved anticancer potential compared to noscapine. We approached to evaluate the single and combined effect of Br-Bn-Nos and docetaxel (DOX) based on molecular modelling and cellular study. The individual predicted free energy of binding ($\Delta G_{bind,pred}$) for Br-Bn-Nos and DOX with tubulin was found to be -28.89 kcal/mol and -36.07 kcal/mol based on MM-GBSA as well as -26.21 kcal/mol and -34.65 kcal/mol based on MM-PBSA, respectively. However, the $\Delta G_{bind,pred}$ of Br-Bn-Nos was significantly reduced (-33.02 kcal/mol and -30.24 kcal/mol using MM-GBSA and MM-PBSA) in presence of DOX on its binding pocket. Parenthetically, the $\Delta G_{bind,pred}$ of DOX was significantly reduced (-37.17 kcal/mol

and -32.80 kcal/mol using MM-GBSA and MM-PBSA) in the presence of Br-Bn-Nos on its binding pocket. The reduced $\Delta G_{bind,pred}$ in presence of Br-Bn-Nos and DOX together indicated a combination effect of both the ligands. The combined interaction of both the agents onto tubulin dimmer was also determined experimentally using purified tubulin, in which a combination regimen of Br-Bn-Nos and DOX reduced the fluorescence intensity of tubulin to a higher value (68%) compared to the single regimen. Further, isobologram analysis revealed the synergistic effect of Br-Bn-Nos and DOX in anti-proliferative activity using MCF-7 cell line at 48 h (sum FIC = 0.49) and at 72 h (sum FIC = 0.62). The combination dose regimen of Br-Bn-Nos and DOX blocks the cell cycle progression at the G2/M phase and induced apoptosis to cancer cells more effectively compared to the single regimen. Taken together, our study provides compelling evidence that the anticancer potential of noscapine derivatives may be substantially improved when it is used in a combined application with DOX for breast cancer.

Keywords: N-3-Br benzyl Noscapine, Molecular Docking, Combination therapy, Docetaxel, Breast cancer, Isobologram

Introduction

Chemotherapeutics regimens currently available for breast cancer have been hindered by poor selectivity towards cancerous cells and hence, associated with severe toxicity (Pace et al. 1996; Rowinsky, 1997; Crown and O'Leary, 2000; Theiss and Meller, 2000; Topp et al. 2000). Over the past few decades, these inadequate scenarios have pushed extensive research on finding more specific and less toxic drugs for cancer. Noscapine, a safe anti-tussive agent, is an excellent choice for cancer treatment because of its mechanism of action, which is not detrimental to healthy cells (Ye et al. 1996; Zhou et al. 2006). It doesn't significantly alter tubulin's stable monomer/polymer ratio over a broad range of concentrations (Ye et al. 1996; Zhou et al. 2003). This is a distinct benefit over currently available antimicrotubule medications, which either prevent microtubule disassembly (taxanes, epothilone) or tubulin assembly (vincas, eribulin, estramustine) and thus do not cause hemo and neuronal toxicity due to its inherent mechanism of action. To optimize its anticancer activity, we strategically developed more effective derivatives by changing the scaffold structure for therapeutics applications. A battery of noscapinoids has already developed, some of which have shown impressive anticancer activity in comparison to noscapine (Naik et al. 2011; Naik et al. 2012; Manchukonda et al. 2013; Manchukonda et al. 2014; Santoshi et al. 2015; Mahaddalkar et al. 2017). However, complete remission of cancer cells was not achieved even at a higher concentration based on *in vivo* animal study (Zhou et al. 2003;

2006). Therefore, new treatment modalities such as combination therapy could be beneficial for breast cancer.

The combination therapy of anti-microtubule agents is an undiscovered source of chemotherapeutic resources. Presence of multiple drug binding sites on the tubulin, suggests that a reasonable combination of two or more drugs of this class may increase the efficacy of anticancer drugs and diminish toxic side effects, thereby improving the therapeutic index. In this study, we approach to evaluate the combined effect of N-3-Br-Benzyl-noscapine and docetaxel towards better anticancer activity. The drug combination significantly reduces the cancer cell growth (sum FIC <1), which shows the synergism between N-3-Br-Benzyl-noscapine and docetaxel in their anticancer activity.

Materials and methods

A. Molecular modeling evaluation of N-3-Br-Benzyl Noscapine as tubulin binding agent and having combination effect with docetaxel

(a) Ligand preparation

The molecular structure of Br-Bn-Nos and docetaxel (DOX) were built using maestro molecular builder (Schrodinger). The constructed structures were energy minimized using Macromodel (version 17.4, Schrodinger) and OPLS 2005 force field. A PRCG algorithm with 1000 steps and an energy gradient of 0.001 was used for energy minimization. Using Ligprep, a suitable bond order was allocated to each ligand. In addition, the ligands were DFT optimized using Jaguar (version 17.4, Schrödinger, LLC) applying Becke's three-parameter exchange potential and the Lee-Yang-Parr correlation functional (B3LYP) (Lee et al. 1988; Becke, 1993) with a basis set 3-21G*(Binkley et al. 1980; Gordon et al. 1982). The various conformations of the molecules were generated using Ligprep (Schrodinger).

(b) Protein preparation

The co-crystal structure of amino-noscapine and tubulin (PDB ID: 6Y6D, resolution 2.20 Å) (Oliva et al. 2020) was used for the molecular docking and predicting the binding affinity of Br-Bn-Nos and DOX. The hydrogen atoms were added and the protein structure was prepared based on the multistep procedure of the protein preparation wizard (Schrodinger). Briefly, it involves minimization of added hydrogen atoms and optimization of hydrogen bonding networks. Further, refinement of the structure was achieved by molecular dynamic simulation of 100 ns

using GROMACS 5.1.5 with similar parameters setting as reported earlier (Santoshi and Naik, 2014).

(c) Molecular docking

The various conformations of Br-Bn-Nos generated above were docked onto the noscapinoids binding site (Oliva et al. 2020) at the interface of αβ-tubulin heterodimer (PDB ID: 6Y6D) prepared above. The binding site was specified by creating two grid boxes around it. An inner grid box of size 14Å x 14Å x 14Å was defined at the centroid of the noscapinoids binding site by selecting the co-complex ligand, amino-noscapine using the Glide grid-receptor generation program. This box defines the search space in which the diameter midpoint of each docked ligand is required to be present. Further, an outer grid box was also defined with a size of ≤ 24 Å of the co-complexed ligand, amino noscapine. It defines the volume within which all ligand atoms of a valid pose must be located. Similarly, the various conformations of the DOX generated above were docked onto the paclitaxel binding site of tubulin reported earlier (Nogales et al. 1998; Synder et al.2000; Canales et al. 2011; Winefield et al.2008). We have used the published co-crystal structure of paclitaxel-tubulin (PDB ID: 1TUB) (Nogales et al. 1998) to extract the binding site amino acids and their coordinates and mapped onto the above prepared protein structure using SiteMap (Schrodinger software package) to define the taxotere binding site. Further, this binding site was specified in the docking of DOX by creating two grid boxes using the grid receptor generation program (Schrodinger software package). An inner grid box of size 14Å x 14Å x 14Å was created at the centroid of the taxotere binding site to define the search space in which the diameter midpoint of each docked ligand is required to be present. Further, an outer grid box with a size of 20Å x 20Å x 20Å was defined within which all ligand atoms of a valid pose must be located. For the molecule docking of Br-Bn-Nos and DOX onto their respective sites we have used Glide-XP algorithm (Halgren et al. 2004) using Schrodinger package and evaluated their binding poses using Glide XP_{Score} function (Friesner et al. 2004; Halgren et al. 2004). Three cycles of molecular docking were performed to elucidate their binding affinity in single as well as in their combination. In the first cycle, both the ligands were docked individually into their respective binding site. In the second cycle, to the co-complex of Br-Bn-Nos and tubulin, DOX was docked to determine the combined effect of DOX with Br-Bn-Nos. Similarly, in the third cycle, to the co-complex of DOX and tubulin, Br-Bn-Nos was docked to determine its combination effect with

docetaxel. For the ligand docking method, the scale factor of 0.4 for van der Waals radii was implemented to protein atoms with exact partial charges less than or equal to 0.25. Out of the 10000 poses sampled, 1000 were extracted by minimization (conjugate gradients) and favorable Glide docking performance was further evaluated by 30 structures with the lowest energy conformation. The single best conformation for each ligand was used for further analysis.

(d) Molecular dynamics simulation

The docked complex of (a) Br-Bn-Nos with tubulin, (b) DOX with tubulin, (c) both Br-Bn-Nos and DOX in combination with tubulin, and (d) the tubulin only was considered for the MD simulation using Amber 16 (Case et al. 2016). The parameters for both the ligands including DOX and Br-Bn-Nos along with GTP and GDP were calculated using Amber 16 software Antechamber system (Wang et al. 2006). All charges for atomic points were determined using the charging model AM1-BCC (Jakalian et al. 2002). In Amber16, topologies and internal coordinates were created for all complexes using tleap programme. Missing hydrogen was added, and Protein and Ligand parameters were assigned using FF14SB and GAFF force fields, respectively (Maier et al. 2015). TIP3P water model in a truncated octahedron at 12 Å distance between the protein atoms and the wall of the box (Jorgensen et al. 1983) was added with dissolved counter ions to neutralize the system. Once the topologies and internal coordinates for all complexes have been obtained, three rounds of minimization have been carried out for each complex in order to relax the system. Position constraints of 10 kcal/Å^2 and 2 kcal/Å^2 have been imposed on the protein system for the first and second rounds, respectively, to relax the water molecules around the protein. In the third round, no restrictions were imposed. After removal of bad contacts through minimization, all four molecular systems were balanced at 300 K and 1 atm at 500 ps. The balanced systems were then run at 100 ns each with a time step of 2 fs. The cut-off for non-bonded interaction was 10 Å during simulations, electrostatics was measured using Particle Mesh Ewald (PME) and bonds were restricted using shake algorithm (Ryckaert et al. 1977; Darden et al. 1993; Essmann et al. 1995). The simulation temperature was regulated with the Langevin thermostat. Coordinates for each molecular system were written every 20 ps.

(e) Predicted free energy of binding using MM-GBSA and MM-PBSA

The predicted free energy of binding ($\Delta G_{bind,pred}$) of Br-Bn-Nos and DOX in their single binding and in co-binding with tubulin was determined as the ensemble average of the binding free energy of a total of 250 snapshots from the last 5 ns of the MD simulation trajectory of their respective molecular systems. We have used molecular mechanics generalized Born solvation area

(MM-GBSA) and molecular mechanics Poisson Boltzmann solvation area (MM-PBSA) methods (Kollman et al. 2000; Massova and Kollman, 2000) to obtain $\Delta G_{bind,pred}$ as explained below:

$\Delta G_{bind,pred} = \Delta G_{complex} - [\Delta G_{Rec} + \Delta G_{lig}]$

$G = E_{gas} + G_{sol} - TS.$

$E_{gas} = E_{int} + E_{ele} + E_{vdw}$

$G_{sol} = G_{PB(GB)} + G_{sol-np}$

$G_{sol-np} = \gamma SAS$

Where, G is Gibbs free energy, E_{gas} is the gas phase energy calculated as the sum of internal energy (E_{int}), energy generated as a result of the electrostatic interaction (E_{ele}) and the van der Waals interaction (E_{vdw}). G_{sol} is the solvation free energy calculated as the sum of polar ($G_{PB(GB)}$) and nonpolar contributions (G_{sol-np}). Polar interaction contribution ($G_{PB(GB)}$) was calculated as the summation of electrostatic contribution (E_{ele}) and polar solvation contribution ($G_{PB(GB)}$). The nonpolar solvation contribution (G_{sol-np}) is approximated as linearly dependent on the solvent accessible surface area (SAS) and γ is the surface tension constant that was set to 0.0072 kcal mol^{-1} $Å^{-2}$ (Massova and Kollman, 2000).

B. Biology

(a) Cell lines and Chemicals

Noscapine and docetaxel were purchased from Sigma. The novel derivative of noscapine, Br-Bn-Nos was chemically synthesized by reaction scheme mentioned below (Manchukonda et al., 2013) and HPLC purified (purity > 96%). The human breast cancer cell line MCF-7 was acquired from the cell registry of the National Centre for Cell Science in Pune, Maharashtra, India. All the chemical reagents and media used for cell culture were obtained from Mediatech, Cellgro. The cells were grown in a 5% CO_2 and 95% humidity in Dulbecco's modified Eagle medium (DMEM, Pan Biotech) at a favorable temperature of 37 °C, supplemented with 10 % fetal bovine serum (FBS) and antibiotics. For bioassays using trypsin-EDTA (0.25%), having a confluence with 70-80 % cells were sub cultured. Cell at 70-80% confluence was sub-cultured using trypsin-EDTA (0.25%) for assays.

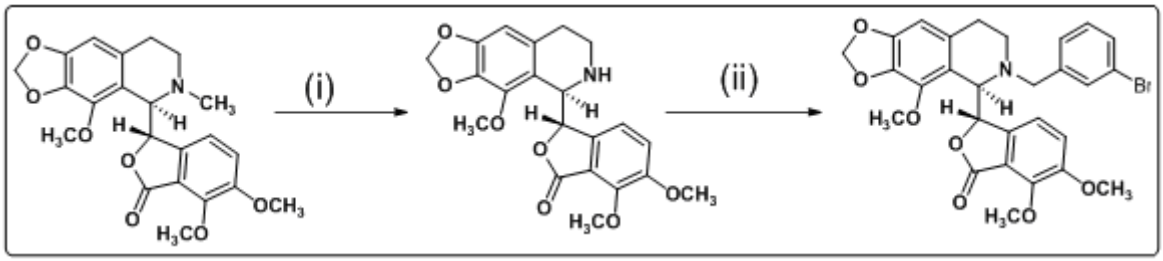

Reaction Scheme: Synthesis of N-3-Br benzyl noscapine: (i) a: *m*-CPBA, DCM; b: 2N HCl; C: $FeSO_4.7H_2O$; (ii) 3-Bromo benzyl bromide, KI, K_2CO_3, Acetone, RT, 97%.

(b) Cell viability assay

The cell proliferation analysis was conducted in 96-well plates using a human breast cancer cell line, MCF-7 at a density of 3 X 10^3 cells/well. The assay was performed with Br-Bn-Nos at variable concentrations of 5, 10, 25, and 50 µM. Similarly, the cells were incubated with DOX at a variable concentration of 0.001, 0.01, 0.1 and 1 µM. After 24 h and 48 h of treatment, the viability of the cell was checked by 3-(4, 5-dimethylthiazol-2-yl)-2, 5, ditetrazolium bromide (MTT) assay. The plate was read at a wavelength of 570 nm in a (Varioskan, Thermo Scientific) flash multimode reader. Fifty percent inhibitory concentration (IC_{50}) of tested drugs was obtained by transferring the data into a graphic program (e.g., Excel) and expressed as a percentage of the untreated controls and then evaluated by Logit regression analysis using a pre-programmed excel spreadsheet obtained from MMV group at Swiss Tropical Institute, Basel, Switzerland (Pandey et al. 2016).

(c) *In vitro* interaction of N-3-Br-Benzyl-noscapine and docetaxel

The cells were treated with a combination regimen of both Br-Bn-Nos and DOX by taking variable concentrations (50 µM Br-Bn-Nos+0.001µM DOX, 25 µM Br-Bn-Nos+0.01 µM DOX, 10 µM Br-Bn-Nos+0.1 µM DOX and 5 µM Br-Bn-Nos+1 µM DOX) directly onto the medium after 12h of cell attachment. The first and the last of these preparations had either Br-Bn-Nos or DOX alone. The cancer cells, MCF-7 at a density of 3 X 10^3 cells/well were exposed for 48 h and 72 h to these dilutions followed by MTT assay. The IC_{50} was determined by logit regression analysis. The fractional inhibitory concentration (FIC) was interpreted by the following formula:

$$FIC = \frac{Conc.of\ drug\ in\ combination\ to\ produce\ IC_{50}}{Conc.\ of\ drug\ alone\ require\ to\ produce\ IC_{50}}$$

The sum FIC value for each of the preparations determined by the following formula was used to classify the drug–drug interaction.

$$Sum\ FIC = \frac{IC_{50}\ of\ drug\ A\ in\ combination}{IC_{50}\ of\ drug\ A\ alone} + \frac{IC_{50}\ drug\ B\ in\ combination}{IC_{50}\ of\ drug\ B\ alone}$$

Sum FIC < 0.5 represents substantial synergism, sum FIC < 1 represents synergism, sum FIC = 1 represents additive interaction, sum FIC ≥ 1 represents antagonism. An Isobologram was plotted to show the drug interaction as per the method proposed earlier (Pandey et al. 2016).

(d) Cell cycle analysis

In Dulbecco's Modification of Eagle's Medium (DMEM), MCF7 cells were cultivated with 4.5 g/l glucose and L-glutamine, supplemented by 10% bovine fetal serum and 1% penicillin/streptomycin. MCF-7 cells ($1X10^5$) were seeded in a 6-well culture plate overnight and then treated with the indicated concentration of Br-Bn-Nos (20 μm) and DOX alone (0.1 μm) and combination regimen (25 μm Br-Bn-Nos+0.01 μm DOX). Staining solution RNase (5μg/ml), propidium iodide (5 μg/ml) and Triton X (0.1%) were used to determine the cell cycle phase and analyzed by flow cytometer (FACS Calibur) to estimate the percentage of cells in the different stages of the cell cycle. The experiment was performed in triplicates.

(e) Annexin V apoptosis assay

Choline phospholipids, like the phosphatidylcholine and sphingomyelin (PS), are subjected on the outer leaflet throughout apoptosis, whereas amino phospholipids (phosphatidylserine, phosphatidylethanolamine) are only found on the cytoplasmic edge of the lipid bilayer. Detection of PS by fluorochrome-tagged 36 KDa anticoagulant protein Annexin V allows for accurate estimation of apoptotic incidence. MCF-7 cells ($5 X 10^4$) were treated with Br-Bn-Nos (20 μm), DOX (0.1 μm) or in their combination regimen (25 μm Br-Bn-Nos+0.01 μm DOX) for apoptosis study using the Annexin V (BD Pharmingen, San Diego, CA, USA) binding assay according to the manufacturer's instructions. The cells were then analyzed using the BD FACS Calibur (San Jose, CA, USA).

(f) Tubulin purification

Two cycles of temperature- and GTP-dependent polymerization and depolymerization in the presence of 1 M glutamate were used to isolate microtubules from the goat brain (Hamel and Lin, 1981). Purified tubulin was extracted from the microtubule proteins by phosphocellulose chromatography based on the methods and procedures discussed earlier (Panda et al. 2000; Joshi and Zohu, 2001) and the amount of purified tubulin was estimated using the Bradford method as well as by SDS PAGE (Bradford, 1976). Aliquots were frozen in liquid nitrogen and preserved at -80 degrees Celsius until required.

(g) Tryptophan fluorescence quenching assay with purified tubulin

Tubulin (2 μM) was treated with desired concentrations of Br-Bn-Nos (20 μM and 50 μM), DOX (0.1 μM) and in combination regimen (DOX 0.01 μM+Br-Bn-Nos 25 μM) in a water bath (35 °C; 45 min). They were then excited at 295 nm and the emission reading at 310–400 nm was

obtained. A FlouroMax® 4 spectrofuorometer (Horiba Scientifc, Edison, NJ) supported by FluorEssence 3.5 software was used for the spectrofluorimetric titrations.

(h) ANS binding assay with purified tubulin

Fluorescence probe 8-anilino-1-napththalene sulfonate (ANS) is mostly used for the detection and analysis of conformational changes in proteins. Tubulin (2 μM) was incubated with 25 μM concentrations of Br-Bn-Nos, 0.1 μM concentration of DOX and in their combination regimen (DOX 0.01 μM+Br-Bn-Nos 25 μM) for 30 min at 35 °C in PEM buffer. ANS (50 μM) was then added to the samples and the samples were incubated in the dark (15 min; 25 °C). After the incubation, they were excited at 350 nm and the emission spectra were taken at 410–470 nm using a Flourolog 3 spectrofluorometer (Horiba Scientific, Edition, NJ) assisted by fluorescence 3.5 software. The assays were repeated two times.

Results

In a quest of increasing the anticancer activity of the noscapine, the –NCH3 group of isoquinoline ring has been substituted with various functional groups based on *in silico* combinatorial approach and screened out potent derivatives for chemical synthesis and experimental evaluation (Manchukonda et al. 2013). Many of these derivatives have shown anticancer activity at a lower concentration compared to noscapine. One of such derivative, N-3-Br-Benzyl noscapine has revealed higher tubulin binding affinity compared to noscapine (Manchukonda et al. 2013) and showed anti-proliferative activity using MDA-MB-231 breast cancer cell line (Cheriyamundath et al. 2019). This derivative of noscapine is different from the first generation noscapine derivatives (including 9-Br-noscapine) in which modification have been done at C-9 position of the isoquinoline ring (Figure 1A,B). Here in this study, we have used N-3-Br-Benzyl derivative of noscapine (Figure 1C) to evaluate its combined effect with docetaxel towards better therapeutic outcome by minimizing the concentration of docetaxel to preclude its side effect.

B. (a) Molecular modelling

In order to determine the predictive binding affinity of Br-Bn-Nos and DOX individually and in their combination, we have docked them at their respective binding pockets on tubulin in three cycles of molecular docking. In the first cycle, DOX and Br-Bn-Nos were docked into their respective binding pockets independently. Both Br-Bn-Nos and DOX docked well into their

binding site with a docking score of -4.99 and -5.88 kcal/mol respectively (Table 1). In the second cycle, the co-complex of tubulin-DOX was taken and Br-Bn-Nos was docked onto its binding site to determine the change in docking score in presence of DOX. The docking score of Br-Bn-Nos was reduced to -6.03 kcal/mol, indicating improvement in its binding affinity in presence of DOX. Similarly in the third cycle, DOX was docked into its binding site in the co-complex of tubulin-Br-Bn-Nos to determine its change in docking score in presence of Br-Bn-Nos. The presence of Br-Bn-Nos further reduced the docking score of DOX to -6.54 kcal/mol. The reduced docking score in presence of Br-Bn-Nos and DOX together indicated the combined effect of both the ligands.

Table 1: Molecular docking results (Glide XP_{score}) and the relevent energy parameters of Br-Bn-Nos and DOX in single as well as in combination with tubulin.

Ligands	Glide XP_{score} (kcal/mol)	Glide E_{vdw} (kcal/mol)	Glide E_{coul} (kcal/mol)	Glide Energy (kcal/mol)
Br-Bn-Nos	-4.99	-31.67	-8.29	-35.97
DOX	-5.88	-42.26	-11.96	-50.22
Br-Bn-Nos docked with Tubulin_DOX complex	-6.03	-39.07	-5.46	-52.53
DOX docked with Tubulin_ Br-Bn-Nos complex	-6.54	-41.24	-9.23	-59.24

(b) MD simulation of the complex

The binding of both Br-Bn-Nos and DOX with tubulin were evaluated independently (Tub-Br-Bn-Nos and Tub-DOX complexes) as well as in combination with tubulin (Tub-DOX+Br-Bn-Nos) by a molecular dynamic simulation of 100 ns. To analyse the system's stability, the root means square deviations (RMSD) of Cα-atoms were computed for all frames over the entire duration of simulation (Figure 2). The fluctuation in the RMSD of Cα carbon atoms was very small after equilibration and all of the systems were found to be stable after 20 ns of simulation. The root mean square fluctuations (RMSF) of Cα-atoms were also measured to see if there were any changes in residue flexibilities during the entire duration of MD simulation (Figure 3). The residues with higher RMSF tend to show more flexibility. Both Br-Bn-Nos and DOX were found to bind with tubulin during the entire duration of the simulation. However, the topmost five ligand-tubulin complexes based on the lowest total energy from the MD simulation trajectory were

obtained to generate the average structure in order to analyze the binding mode of ligands. Both Br-Bn-Nos and DOX were found to accommodate well inside the binding cavity. The Br-Bn-Nos docked well at the interface of α- and β- tubulin, whereas the binding of DOX is biased more towards β-tubulin (Figure 4a, b). Their binding mode with the tubulin was represented by ligplots in single as well as in combination (Figure 5a-d). The binding site amino acids involved in the binding of Br-Bn-Nos independently and in the presence of DOX were found albite different, which may be due to the change in conformation of tubulin in presence of DOX. None of the binding site amino acids were involved in hydrogen bonding with the Br-Bn-Nos when it was docked individually onto tubulin (Figure 5a). In contrast, the binding site amino acids Asp 357(D), Cys 356(D), Cys 241(D), and Gln 247(D) were involved in making 6 hydrogen bonding with Br-Bn-Nos in presence of DOX (Figure 5b). Parenthetically, the binding site amino acids Arg 278(D) and Arg 284(D) are involved in 2 hydrogen bonding with DOX when it was docked individually onto tubulin (Figure 5c). In contrast, the binding site amino acids Gly 370(D), Arg 278(D), Arg 284(D), and Gln 281(D) are involved in making 9 hydrogen bonds with DOX in presence of Br-Bn-Nos (Figure 5d).

(c) Calculated free energy of binding of Br-Bn-Nos and DOX with tubulin

The free energy of binding and its respective components of both Br-Bn-Nos and DOX with tubulin were calculated independently as well as in combination and presented in Table 2. The last 250 frames from the last 5 ns of trajectory were considered to calculate the ensemble average of the free energy of binding using both MM-GBSA and MM-PBSA methods. The free energy of binding for Br-Bn-Nos and DOX with tubulin was found to be -28.89 and -36.07 kcal/mol based on MM-GBSA as well as -26.21 and -34.65 kcal/mol based on MM-PBSA, respectively. Further, the free energy of binding of Br-Bn-Nos was reduced to -33.02 and -30.24 kcal/mol using MM-GBSA and MM-PBSA calculation when DOX was present on its binding pocket, indicating combination effect of both the ligands. Parenthetically, the free energy of binding of DOX was reduced to -37.17 and -32.80 kcal/mol using MM-GBSA and MM-PBSA, respectively when Br-Bn-Nos was present in binding tubulin. For all complexes, the binding energy was decomposed into its various energy components (the electrostatic, van der Waals, and solvation). Both van der Waals (ΔE_{VDW}) and the electrostatic component (ΔE_{ELE}) were observed to make very significant contributions to the free energy of binding. However, the net polar contribution ($\Delta G_{(ele,PB/GB)} = \Delta E_{ele} + \Delta G_{(PB/GB)}$) was rendered unfavorable due to very large penalty

imposed by the desolvation component ($\Delta G_{PB/GB}$) while the net nonpolar component (ΔE_{vdw}) and ($\Delta G_{sol\text{-}np}$) were observed to make a highly favourable contribution to the free energy of binding.

Table 2: Predicted free energy of binding ($\Delta G_{bind,pred}$) and its various componentes (kcal/mol) of Br-Bn-Nos and DOX in single as well as in combination binding with tubulin. The values in bold represent the ($\Delta G_{bind,pred}$ of molecules with tubulin based on MM-GBSA and MM-PBSA methods.

Energy Component	Br-Bn-Nos	Dox	Tub_DOX+ Br-Bn-Nos	Tub_Br-Bn-Nos+ DOX
ΔE_{VDW}	-31.61	-42.26	-41.24	-39.07
ΔE_{ELE}	-286.66	-21.21	-303.55	-30.00
ΔE_{GAS}	-333.46	-57.26	-348.88	-65.40
$\Delta G_{GB\text{-}Polar}$	308.85	39.70	307.49	32.98
$\Delta G_{SOL\text{-}NP}$	-3.62	-4.61	-3.69	-4.65
$\Delta G_{SOL\text{-}GB}$	279.35	29.19	323.90	31.03
$\Delta G_{bind\text{-}GBSA}$	**-28.89**	**-36.07**	**-33.02**	**-37.17**
ΔG_{PB}	323.16	30.62	335.94	36.69
$\Delta G_{SOL\text{-}NP}$	-3.54	-4.51	-3.36	-4.29
$\Delta G_{SOL\text{-}PB}$	279.22	29.61	320.48	33.69
$\Delta G_{bind\text{-}PBSA}$	**-26.21**	**-34.65**	**-30.24**	**-32.80**

B. Biology

(a) Inhibition of cellular proliferation

The Br-Bn-Nos inhibited proliferation of MCF-7 cells in a dose-dependent manner with IC_{50} values of 11.5 μM and 7.71 μM respectively at 48 h and 72 h (Figure 6a). Similarly, the DOX showed IC_{50} values of 0.39 μM and 0.016 μM against MCF-7 cells respectively at 48 h and 72 h (Figure 6b). In order to minimize the toxicity of DOX and to enhance the antiproliferative efficacy we have examined the antiproliferative activity with a combination of a lower concentration of DOX and a higher concentration of Br-Bn-Nos. Approximately, 50% inhibition of cellular proliferation was achieved in a combination regimen of Br-Bn-Nos (5 μM) and DOX (1μM) after 48 h and 72 h post-treatment (Figure 6c). Further, the interaction of both the agents has been analyzed on the basis of their sum FICs and isobologram plot (Figure 7). The sum FICs value was found to be 0.49 and 0.62 respectively at 48 h and 72 h. The isobologram of N-3-Br-Benzyl-

noscapine with docetaxel suggests that the combination has synergistic antiproliferative activity both at 48 h and 72 h exposure (sum FIC <1).

(b) Cell cycle effect

Both noscapinoids and docetaxel have been reported to bind tubulin and inhibit the cell cycle progression at G2/M phase, followed by induction of apoptosis to cancer cells (Ye et al. 1998; Dash et al. 2020). We examined the inhibition in cell cycle progression of MCF-7 cells with the treatment of Br-Bn-Nos and DOX in single as well as in combination regimens. The cells were treated with 20 μM of Br-Bn-Nos and 0.1 μM of DOX in the single regimen, whereas 25 μM Br-Bn-Nos+0.01 μM DOX for the combination regimen. The cell cycle distribution was evaluated via flow cytometric analysis. The presence of 2N DNA indicates that the cells are in the G1 phase, while the accumulation of duplicated 4N DNA indicates that the cells are in G2 and M phases. Accumulation of DNA in between 2N and 4N peaks represent, the cells are in the S phase. In contrast, less than 2N DNA indicates the apoptotic cells in which the DNA is degraded to different extents (sub-G1 phase). As shown in Figure 8, there is a high accumulation of cells in the G2/M phase. In contrast to the G2/M phase block, cells with sub-G1 phase were found to increase compared to the control after 48 h of treatment in single and in a combination regimen. The sub-G1 population with the treatment of Br-Bn-Nos was increased to 15.4%, whereas with DOX it was increased to 16.1% and in combination, it further increased to 23.2% in comparison to control. The combined effect of both Br-Bn-Nos and DOX on cell cycle progression could be useful for the induction of apoptosis.

(c) Induction of apoptosis

Induction of apoptosis to MCF-7 cells was investigated using PE Annexin V and 7-AAD apoptosis kit. The representative dot-plots illustrating apoptotic status was shown in Figure 9. The percentage of apoptotic cells (early apoptotic and late apoptotic cells) treated with Br-Bn-Nos (25 μm) + DOX (0.01 μm) was 24.1% and 20.3%, which was significantly high compared to single regimen treatment with 20 μm of Br-Bn-Nos (11.0 % and 3.73 %) or 0.1 μm of DOX (10.9 % and 3.80 %) respectively after 48h in comparison to controlled untreated cells. This study demonstrated that the proposed combination effect of Br-Bn-Nos and DOX would not only potentially induced apoptosis to the cancer cell, but also provide a promising prospect of order to reduce the toxicity of DOX.

(c) Both Br-Bn-Nos and DOX bind tubulin in single and in combination regimen

In order to experimentally validate our findings based on molecular modelling study with respect to the tubulin-binding affinity of Br-Bn-Nos and DOX in single as well as in their combination, we determined the quenching of fluorescence intensity of tubulin with the treatment of both the agents in single as well as in combination regimen. Due to the presence of the aromatic amino acid tryptophan, the tubulin is autofluorescence in nature. Any chemical compounds that bind with tubulin and alter its conformation leads to a decrease in its intrinsic fluorescence. The relative percentage of decrease in fluorescence intensity was 31.01% with the treatment of 25 μM of Br-Bn-Nos and 58% with the treatment of 0.1 μM of DOX, suggesting that both the agents bind to tubulin with different affinity. Further, the fluorescent intensity of tubulin was reduced to a higher value of 68% with the combination treatment of Br-Bn-Nos (25μM) and DOX (0.1μM) (Figure 10). Significant reduction in tubulin fluorescence intensity in the combination regimen of Br-Bn-Nos and DOX indicate co-binding of both the ligands with tubulin.

(d) Effect of Br-Bn-Nos and DOX on conformational changes of tubulin

In order to further investigate the structural changes on tubulin due to binding of Br-Bn-Nos and DOX in single as well as in combination regimen, we probed the tertiary structure of the protein using an ANS-binding assay. ANS is a fluorescent probe, whose fluorescence improves when attached to protein. ANS, when bound to hydrophobic patches on proteins, shows enhanced fluorescence. An increase in ANS fluorescence of tubulin suggests a loss of protein structural integrity. Purified tubulin with the treatment of Br-Bn-Nos (25μM) and DOX (0.1 μM) showed an increase in tubulin-ANS fluorescence intensity (Figure 11). It displayed a 29.8% increase in fluorescence intensity at 25 μM Br-Bn-Nos, and 40.39% in presence of DOX (0.1 μM) compared to unbound tubulin. Similarly, in combination treatment with Br-Bn-Nos (25 μM) and DOX (0.1 μM) the tubulin-ANS fluorescence intensity was further increased to 57.50% respectively, indicating a gradual incremental perturbation of the structural integrity of the tubulin by the binding of both the agents together.

Discussion

Poor clinical prospects of the current chemotherapy have triggered the development of new treatment modalities such as combination therapy for breast cancer. It is becoming well-appreciated that a toxic drug at its maximum tolerated dose given intermittently is not necessarily better and there exists an opportunity to reduce its dose levels by using combination regimens of drugs that display synergistic interactions (Jordan and Wilson, 2004). The presence of diverse

drug binding sites on tubulin suggests that rational combination of two or more drugs of anti-microbial therapy might be able to enhance the anti-cancer efficacy and reduce toxic side effects, thereby improving the therapeutic index. Tubulin binding drugs such as taxanes and vinca alkaloids are the most efficient anticancer agents for breast cancer treatment (Chougule et al.2011). However, due to the emergence of drug resistance and the subsequent serious side effects, their therapeutic utility is limited (Doddapaneni et al. 2016). In contrast, noscapine, a less toxic orally administered antimicrotubular agent, clearly indicates antitumor activity *in vitro* and *in vivo* against a number of cancers (Laden et al. 2002; Zohu et al.2002; Zhou et al. 2006). Therefore, to decrease the severe side effects of docetaxel and increase its anti-cancer effectiveness we adopt a combination treatment with one of the derivatives of noscapine i.e. Br-Bn-Nos. Similar studies have been conducted previously to demonstrate the combination effect of DOX and other anticancer agents for better therapeutic efficacy (Dash et al. 2020; Galsky and Vogelzang, 2010; Fisusi and Akala, 2019).

In this study, we have demonstrated the combined effect of Br-Bn-Nos and DOX based on molecular modeling and cellular study. Molecular docking of Br-Bn-Nos and DOX, individually, revealed a docking score of -4.99 kcal/mol and -5.88 kcal/mol respectively. However, the docking score of Br-Bn-Nos was significantly reduced (-6.03 kcal/mol) when it was docked onto a co-complex of tubulin-DOX and similarly docking score of DOX was reduced to a greater extent (-6.54 kcal/mol) when it was docked onto a co-complex of tubulin-Br-Bn-Nos, indicating co-binding of both the agents simultaneously to tubulin at two different binding pockets. Further, the significant reduction in free energy of binding based on MD simulation in combination with MM-GBSA and MM-PBSA calculation in presence of Br-Bn-Nos and DOX together compared to their individual binding with tubulin indicated a combination effect of both the ligands. The result obtained from theoretical prediction was validated through experiments by tubulin-binding assay and tubulin-ANS binding assay. Combination treatment of Br-Bn-Nos and DOX reduced the fluorescence intensity of tubulin to a higher value compared to their single regimen treatment, indicating the combined effect of both the agents. Similarly, a significant increase in fluorescent intensity of tubulin-ANS with the treatment of Br-Bn-Nos and DOX in combination regimen compared to single regimen treatment suggest co-binding of both the agents to tubulin. The combined effect of both Br-Bn-Nos and Dox was also revealed from the cellular study using the MCF-7 cancer cell line. Combination treatment of Br-Bn-Nos and DOX was found to be more effective in inhibiting cellular proliferation, blocking of cell cycle progression and induction of

apoptosis compared to single-drug treatment. Further, the isobologram analysis (sum FIC <1) of docetaxel with Br-Bn-Nos indicate significant synergism at 48 h and 72 h exposures.

In conclusion all these results taken together established a proof-of-concept that a rational combination of Br-Bn-Nos and DOX could generate synergistic effects on cancer treatment, which is a highly promising and novel approach for the treatment of breast cancer. Further studies need to be conducted to better understand the growth inhibition molecular mechanism in the combined treatment of breast cancer cells.

Acknowledgments

We would like to acknowledge the financial assistant provided by the Department of Science and Technology, Government of India (Award no- DST/INSPIRE/Code No.: IF170022) for providing student research fellowship to Shruti Gamya Dash and also the financial support by OHEPEE, Govt. of Odisha through World Bank. We are grateful to Dr. Manu Lopus and UM-DAE Centre for Excellence in Basic Sciences for providing extended facilities.

Conflict of Interest

The authors declare no conflict of interest.

REFERENCES

1. Becke, A.D. (1993). A new mixing of Hartree-Fock and local density-functional theories. *Journal of Chemical Physics*, 98, 1372-1377.https://doi:10.1063/1.464304.

2. Binkley, J.S., Pople, J.A., &Hehre, W.J. (1980). Self-consistent molecular orbital methods, Small split-valence basis sets for first-row elements.*Journal of the American Chemical Society*, 102, 939-947. https://doi.org/10.1021/ja00523a008.

3. Bradford, M.M. (1976). A rapid and sensitive method for the quantitation of microgram quantities of protein utilizing the principle of protein-dye binding. *Analytical Biochemistry*, 72, 248-254. https://doi.org/10.1016/0003-2697(76)90527-3.

4. Case, D.A., Betz, R.M., Cerutti, D.S., Cheatham, T.E. III., Darden, T.A., Duke, R.E., Giese, T.J., Gohlke, H., Goetz, A.W., Homeyer, N., Izadi, S., Janowski, P., Kaus, J., Kovalenko, A., Lee, T.S., LeGrand, S., Li, P., Lin, C., Luchko, T., Luo, R., Madej, B., Mermelstein, D., Merz, K.M., Monard, G., Nguyen, H., Nguyen, H.T., Omelyan, I., Onufriev, A., Roe, D.R., Roitberg, A., Sagui, C., Simmerling, C.L., Botello-Smith, W.M., Swails, J., Walker, R.C., Wang, J.,

Wolf, R.M., Wu, X., Xiao, L., &Kollman, P.A. (2016). *AMBER*. 2016. University of California, San Francisco.

5. Canales, A., Rodríguez-Salarichs, J., Trigili, C., Nieto, L., Coderch, C., Andreu, J. M., Paterson, I., Jiménez-Barbero, J., & Díaz, J. F. (2011). Insights into the interaction of discodermolide and docetaxel with tubulin. Mapping the binding sites of microtubule-stabilizing agents by using an integrated NMR and computational approach. *ACS chemical biology*, *6*(8), 789–799. https://doi.org/10.1021/cb200099u.

6. Cheriyamundath, S., Mahaddalkar, T., Reddy Nagireddy, P. K., Sridhar, B., Kantevari, S., & Lopus, M. (2019). Insights into the structure and tubulin-targeted anticancer potential of N-(3-bromobenzyl) noscapine. *Pharmacological reports : PR*, *71*(1), 48–53. https://doi.org/10.1016/j.pharep.2018.09.002.

7. Chougule, M. B., Patel, A. R., Jackson, T., & Singh, M. (2011). Antitumor activity of Noscapine in combination with Doxorubicin in triple negative breast cancer. *PloS one*, *6*(3), e17733. https://doi.org/10.1371/journal.pone.0017733.

8. Crown, J., & O'Leary, M. (2000). The taxanes: an update. *Lancet,* 355, 1176-1178.

9. Darden, T., York, D., & Pedersen, L. (1993). Particle mesh Ewald: An N. log (N) method for Ewald sums in large systems.*Journal of Chemical Physics*, 98, 10089-10092. https://doi.org/10.1063/1.464397

10. Dash, S. G., Suri, C., Nagireddy, P., Kantevari, S., & Naik, P. K. (2020). Rational design of 9-vinyl-phenyl noscapine as potent tubulin binding anticancer agent and evaluation of the effects of its combination on Docetaxel. *Journal of biomolecular structure & dynamics*, 1–14. Advance online publication. https://doi.org/10.1080/07391102.2020.1785945.

11. Doddapaneni, R., Patel, K., Chowdhury, N., & Singh, M. (2016). Noscapine chemosensitization enhances docetaxel anticancer activity and nanocarrier uptake in triple negative breast cancer. *Experimental cell research*, *346*(1), 65–73. https://doi.org/10.1016/j.yexcr.2016.05.006.

12. Essmann, U., Perera, L., Berkowitz, M.L., Darden, T., Lee, H., & Pedersen, L.G. (1995). A Smooth particle mesh: Ewald method. *Journal of Chemical Physics*, *103*, 8577-8593. https://doi.org/10.1063/1.470117.

13. Fisusi, F. A., & Akala, E. O. (2019). Drug Combinations in Breast Cancer Therapy. *Pharmaceutical nanotechnology*, *7*(1), 3–23. https://doi.org/10.2174/2211738507666190122111224.

14. Friesner, R. A., Banks, J. L., Murphy, R. B., Halgren, T. A., Klicic, J. J., Mainz, D. T., Repasky, M. P., Knoll, E. H., Shelley, M., Perry, J. K., Shaw, D. E., Francis, P., & Shenkin, P. S. (2004). Glide: a new approach for rapid, accurate docking and scoring. 1. Method and assessment of docking accuracy. *Journal of medicinal chemistry*, *47*(7), 1739–1749. https://doi.org/10.1021/jm0306430.

15. Galsky, M. D., &Vogelzang, N. J. (2010). Docetaxel-based combination therapy for castration-resistant prostate cancer. *Annals of oncology : official journal of the European Society for Medical Oncology*,21(11), 2135–2144. https://doi.org/10.1093/annonc/mdq050.

16. Gordon, M.S., Binkley, J.S., Pople, J.A., Pietro, W.J., &Hehre, W.J. (1982).Self-consistent molecular-orbital methods. Small split valence basis sets for second-row elements. *Journal of the American Chemical Society*, *104*, 2797-2803. https://doi.org/10.1021/ja00383a007.

17. Halgren, T.A., Murphy, R.B., Friesner, R.A., Beard, H.S., Frye, L.L., Pollard, W.T., & Banks, J.L. (2004). Glide: a new approach for rapid, accurate docking and scoring. 2. Enrichment factors in database screening. *Journal of Medicinal Chemistry*, 47, 1750-1759. https://doi.org/10.1021/jm030644s.

18. Hamel, E., & Lin, C.M. (1981). Glutamate-induced polymerization of tubulin: characteristics of the reaction and application to the large-scale purification of tubulin. *Archives of Biochemistry and Biophysics*, 209, 29-40.https://doi: 10.1016/0003-9861(81)90253-8.

19. Jakalian, A., Jack, D.B., &Bayly, C.I. (2002). Fast, efficient generation of high-quality atomic charges. AM1-BCC model: II. Parameterization and validation. *Journal of Computational Chemistry*, *23*, 1623-1641.https://doi.10.1002/jcc.10128.

20. Jordan, M. A., & Wilson, L. (2004). Microtubules as a target for anticancer drugs. *Nature reviews. Cancer*, *4*(4), 253–265. https://doi.org/10.1038/nrc1317.

21. Jorgensen, W.L., Chandrasekhar, J., Madura, J.D., Impey, R.W., & Klein, M.L. (1983). Comparison of simple potential functions for simulating liquid water. *Journal of Chemical Physics*, 79, 926-935. https://doi.org/10.1063/1.445869.

22. Joshi, H.C., &Zohu, J. (2000). Noscapine and Analogues as Potential Chemotherapeutic Agents. *Drug News & Perspectives,* 13, 543-546.https://doi: 10.1358/dnp.2000.13.9.858482.

23. Joshi, H.C., &Zohu, J. (2001). Gamma tubulin and microtubule nucleation in mammalian cells. *Methods Cell Biology*, 67, 179-193.doi: https://doi.org/10.1016/S0091-679X(01)67013-4.

24. Karlsson, M. O., Dahlstrom, B., Eckernas, S. A., Johansson, M. &Alm, A. T. (1990). Pharmacokinetics of oral noscapine. *European. Journal of Clinical. Pharmacology,* 39, 275–279. https://doi.org/10.1007/BF00315110

25. Kleeberg, U.R., Fink, M. Tessen, H.W., Nennecke, A., Hentschel, S. & Bartels, S. (2013). Adjuvant therapy reduces the benefit of palliative treatment in disseminated breast cancer-own findings and review of the literature. *Onkologie,* 36(6):348-56. doi: 10.1159/000351253.

26. Kollman, P.A., Massova, I., Reyes, C., Kuhn, B., Huo, S., Chong, L., Lee, M., Lee, T., Duan, Y., & Wang, W. (2000). Calculating structures and free energies of complex molecules: combining molecular mechanics and continuum models. *Accounts of Chemical Research*, 33(12), 889-897. doi: 10.1021/ar000033j

27. Lee, C., Yang, W., & Parr, R.G. (1988). Development of the Colle-Salvetti correlation-energy formula into a functional of the electron densityPhysical Review B: Condensed Matter and Materials Physics, 37, 785-789. https://doi: 10.1103/physrevb.37.785.

28. Mahaddalkar, T., Naik, P.K., Choudhary, S., Manchukonda, N., Kantevari, S., &Lopus, M. (2017). Structural investigations into the binding mode of a novel noscapine analogue, 9-(4-vinylphenyl) noscapine, with tubulin by biochemical analyses and molecular dynamic simulations. *Journal of Biomolecular Structure and Dynamics.35*, 2475-2482. https://doi: 10.1080/07391102.2016.1222969.

29. Maier, J.A., Martinez, C., Kasavajhala, K., Wickstrom, L., Hauser, K.E., & Simmerling, C. (2015). ff14SB: Improving the accuracy of protein side chain and backbone parameters from ff99SB. *Journal of Chemical Theory and Computation,11*, 3696-3713. https://doi.org/10.1021/acs.jctc.5b00255.

30. Manchukonda, N.K., Naik, P.K., Santoshi, S., Lopus, M., Joseph, S., Sridhar, B., &Kantevari, S. (2013). Rational design, synthesis and biological evaluation of third generation α-noscapine analogues as potent tubulin binding anticancer agents. *PLoS One.*, *8*, e77970.https://doi: 10.1371/journal.pone.0077970.

31. Manchukonda, N.K., Naik, P.K., Sridhar, B., &Kantevari, S. (2014). Synthesis and biological evaluation of novel biaryl type α-noscapine congeners. B*ioorganic & Medicinal Chemistry Letters*. 24, 5752-5757.

32. Massova, I., & Kollman, P.A. (2000). Combined molecular mechanical and continuum solvent approach (MM-PBSA/GBSA) to predict ligand binding. *Perspectives in Drug Discovery and Design*, 18(1), 113-135.

33. Naik, P.K., Chatterji, B.P., Vangapandu, S.N., Aneja, R., Chandra, R., Kanteveri, S., & Joshi, H.C. (2011). Rational design, synthesis and biological evaluations of amino-noscapine: a high affinity tubulin-binding noscapinoid. *Journal of Computer-Aided Molecular Design,* 25, 443-454. https://doi: 10.1007/s10822-011-9430-4.

34. Naik, P.K., Lopus, M., Aneja, R., Vangapandu, S.N., & Joshi, H.C. (2012). *Insilico* inspired design and synthesis of a novel tubulin-binding anti-cancer drug: folate conjugated noscapine (Targetin). *Journal of Computer-Aided Molecular Design*, 26, 233–247.

35. Naik, P.K., Santoshi, S., Rai, A., & Joshi, H.C. (2011). Molecular modelling and competition binding study of Br-noscapine and colchicine provide insight into noscapinoid-tubulin binding site. *Journal of Molecular Graphics and Modelling*, 29, 947-955.https://doi: 10.1016/j.jmgm.2011.03.004.

36. Nogales, E., Wolf, S. G., & Downing, K. H. (1998). Structure of the alpha beta tubulin dimer by electron crystallography. *Nature*, *391*(6663), 199–203. https://doi.org/10.1038/34465.

37. Oliva, M.A., Prota, A.E., Rodríguez-Salarichs, J., Bennani, Y.L., Jiménez-Barbero, J., Bargsten, K., Canales, A., Steinmetz, M.O., & Diaz, J.F. (2020). Structural basis of noscapine activation for tubulin binding. *Journal of Medicinal Chemistry*, 63, 8495-8501.https://doi.10.1021/acs.jmedchem.0c00855.

38. Pace, A., Bove, L., Nistico, C., Ranuzzi, M., Innocenti, P., Pietrangeli, A., Terzoli, E., &Jandolo, B. (1996). Vinorelbine neurotoxicity: clinical and neurophysiological findings in 23 patients. *Journal of Neuropsychology.*, 61, 409-411. https://doi:10.1136/jnnp.61.4.409.

39. Panda, D., Chakrabarti, G., Hudson, J., Pigg, K., Miller, H.P., Wilson, L., & Himes, R.H. (2000). Suppression of microtubule dynamic instability and treadmilling by deuterium oxide. *Journal of Biochemistry,* 39, 5075-5081. https://doi.org/10.1021/bi992217f.

40. Pandey, S.K, Biswas, S., Gunjan, S., Chauhan, B.S., Singh, S.K., Srivastava, K., Singh, S., Batra, S., Tripathi, R., (2016). Pyrrolidine-Acridine hybrid in Artemisinin-based combination: a pharmacodynamic study. *Parasitology*, 143(11), 1421-32. doi: 10.1017/S0031182016000937.

41. Rowinsky, E.K. (1997). The development and clinical utility of the taxane class of antimicrotubule chemotherapy agents. *Annual Review of Medicine*, 48, 353-374. https://doi:10.1146/annurev.med.48.1.353.

42. Ryckaert, J.P., Ciccotti, G., & Berendsen, H.J. (1977). Numerical integration of the cartesian equations of motion of a system with constraints: molecular dynamics ofn-alkanes. *Journal of Computational Physics,* 23, 327-341. https://doi.org/10.1016/0021-9991(77)90098-5.

43. Santoshi, S., & Naik, P.K. (2014). Molecular insight of isotypes specific β-tublin interaction of tubulin heterodimer with noscapinoids. *Journal of Computer-Aided Molecular Design*, *28*, 751-763. https://doi.10.1007/s10822-014-9756-9.

44. Santoshi, S., Manchukonda, N.K., Suri, C., Sharma, M., Sridhar, B., Joseph, S., Lopus, M., Kantevari, S., Baitharu, I., & Naik, P.K. (2015). Rational design of biaryl pharmacophore inserted noscapine derivatives as potent tubulin binding anticancer agents. *Journal of Computer aided Molecular Design*, 29, 249-270.https://doi: 10.1007/s10822-014-9820-5.

45. Snyder, J. P., Nettles, J. H., Cornett, B., Downing, K. H., & Nogales, E. (2001). The binding conformation of Taxol in beta-tubulin: a model based on electron crystallographic density. *Proceedings of the National Academy of Sciences of the United States of America*, *98*(9), 5312–5316. https://doi.org/10.1073/pnas.051309398.

46. Theiss, C., &Meller, K. (2000). Taxol impairs anterograde axonal transport of microinjected horseradish peroxidase in dorsal root ganglia neurons in vitro. *Cell Tissue Research*, 299 213-224. https://doi: 10.1007/s004419900120.

47. Topp, K.S., Tanner, K.D., & Levine, J.D. (2000). Damage to the cytoskeleton of large diameter sensory neurons and myelinated axons in vincristine-induced painful peripheral neuropathy in the rat. *ournal of Comparative Neurology*, 424, 563-576

48. Wang, J., Wang, W., Kollman, P.A., & Case, D.A. (2006). Automatic atom type and bond type perception in molecular mechanical calculations.*Journal of Molecular Graphics and Modelling,* 25, 247-260.

49. Winefield, R. D., Entwistle, R. A., Foland, T. B., Lushington, G. H., & Himes, R. H. (2008). Differences in paclitaxel and docetaxel interactions with tubulin detected by mutagenesis of yeast tubulin. *ChemMedChem*, *3*(12), 1844–1847. https://doi.org/10.1002/cmdc.200800288.

50. Y. Ke., K. Ye., Grossniklaus, H.E., Archer, D.R., Joshi, H.C., & Kapp, J.A. (2000). Noscapine inhibits tumor growth with little toxicity to normal tissues or inhibition of immune responses. *Cancer Immunology, Immunotherapy*, 49, 217-225. https://doi: 10.1007/s002620000109.

51. Ye, K., Ke, Y., Keshava, N., Shanks, J., Kapp, J.A., Tekmal, R.R., Petros, J., & Joshi, H.C. (1998). Opium alkaloid noscapine is an antitumor agent that arrests metaphase and induces apoptosis in dividing cells. *Proceedings of the NationalAcademy of Sciences of the United States of America,* 95, 1601-1606.doi: https://doi.org/10.1073/pnas.95.4.1601.

52. Zhou, J., Gupta, K., Aggarwal, S., Aneja, R., Chandra, R., Panda, D., & Joshi, H.C. (2003). Brominated derivatives of noscapine are potent microtubule-interfering agents that perturb mitosis and inhibit cell proliferation. *Molecular Pharmaceutics*, 63, 799-807. https://doi: 10.1124/mol.63.4.799.

53. Zhou, J., Gupta, K., Yao, J., Ye, K., Panda, D., Giannakakou, P., & Joshi, H. C. (2002). Paclitaxel-resistant human ovarian cancer cells undergo c-Jun NH2-terminal kinase-mediated apoptosis in response to noscapine. *The Journal of biological chemistry*, *277*(42), 39777–39785. https://doi.org/10.1074/jbc.M203927200

54. Zhou, J., Liu, M., Aneja, R., Chandra, R., Lage, H., & Joshi, H.C. (2006). Reversal of P glycoprotein mediated multidrug resistance in cancer cells by the c-jun NH2-terrminal kinase. *Cancer Research,* 66, 445-452. https://doi: 10.1158/0008-5472.CAN-05-1779.

Legends of Figures

Figure 1: Structures of the (A) first generation noscapinoids that identifies the 9th position modification in the noscapine scaffold, (B) molecular structure of the 9-Br-Noscapine and (C) N-3-Br Benzyl Noscapine.

Figure 2: Root mean square deviations (RMSD) of Cα carbon atoms of tubulin only and in complex with Br-Bn-Nos (Tubulin+ Br-Bn-Nos), with docetaxel (Tubulin+DOX) and with both docetaxel and Br-Bn-Nos (Tubulin+DOX+Br-Bn-Nos) during 100 ns of MD simulation. The relative fluctuation in the RMSD of the Cα atoms is very small after ~ 20 ns of the simulation. The time step of 20 ps was used during the simulation. The topmost 5 frames from the MD simulation trajectory with lowest total energy were considered to generate the average structure.

Figure 3: Root mean square fluctuation (RMSF) of the residues of tubulin of the docked ligands in the bound form and in the unbound form of tubulin heterodimer. Different levels of flexibility of these residues were noticed in the bound form of tubulin with Br-Bn-Nos and DOX in single as well as in combination. Most of the residues showed flexibilities >5 Å in case of tubulin bound with Br-Bn-Nos and DOX as compared to the free tubulin heterodimer, indicating that these residues seem to be more flexible as a result of binding.

Figure 4. (a) Both Br-Bn-Nos and DOX are well accomodated inside their respective binding site of tubulin. (b) Snapshot of both the ligands obtained. The binding site is represented as

macromodel surface according to α- and β- tubulin (α-tubulin is represented in blue colour and β-tubulin is represented in brown colour).

Figure 5. The ligplot analysis showing the binding mode of (a) Br-Bn-Nos with tubulin, (b) Br-Bn-Nos with the co-complex of Tubulin-DOX, (c) DOX with tubulin, and (d) DOX with the co-omplex of tubulin-Br-Bn-Nos. The binding mode of Br-Bn-Nos was different when docked to tubulin and to the co-complex of tubulin-DOX, in which different number of hydrogen bondings were involved with the binding site amino acids. Similarly, the binding mode of DOX was also different when docked to tubulin and to the co-complex of tubulin-Br-Bn-Nos, in which different number of hydrogen bonding involved with the binding site amino acids. The hydrogen bonds formed (if any) are represented as dotted lines and the value represents the bond distance.

Figure 6. Br-Bn-Nos and DOX in single as well as in combination regimen at different concentrations inhibit cellular proliferation of human breast cancer cell, MCF-7 after 48 h and 72 h treatment. The IC_{50} value amounted to 11.5 μM and 7.71 μM, respectively for 48h and 72h with Br-Bn-Nos. Similarly, the IC_{50} value amounted to 0.39 μM and 0.016 μM, respectively for 48h and 72h with DOX. In contrast, approximately 50% inhibition of cellular inhibition was achieved in a combination regimen of Br-Bn-Nos (5μM) and DOX (0.001μM) after 48 h and 72 h post-treatment.

Figure 7. Isobolograms showing *in vitro* interactions between Br-Bn-Nos and DOX. Sum FIC < 0.5 represents substantial synergism, sum FIC < 1 represents synergism, sum FIC = 1 represents additive interaction, and sum FIC >1 represents antagonism between two drugs.

Figure 8. Figure A-D depict represented figures of analyses of cell cycle distribution in a two-dimensional disposition as determined by flow cytometry in MCF-7 cells treated with 20 μM of Br-Bn-Nos, 0.1 μM of DOX as single regimen and 25 μM of Br-Bn-Nos + 0.01 μM of DOX in combination regimen. Both Br-Bn-Nos and DOX inhibit cell cycle progression at mitosis followed by the appearance of a characteristic hypodiploid (sub-G1) DNA peak, indicative of apoptosis.

Figure 9. Analysis of apoptosis cell death induced by Br-Bn-Nos alone and in combination with DOX based on flow cytometric analysis. PE conjugate of Annexin V was used in combination

with 7-Amino-Actinomycin (7-AAD) to distinguish among 3 subpopulations: PE^{--} and 7-AAD^{--} population indicates viable cells (bottom left quadrant); PE^{--} and 7-AAD^{+} population indicates early apoptotic cells (lower right quadrant); PE^{+} and 7-AAD^{+} population indicate late apoptotic cells (top right quadrant).

Figure 10. Decrease of fluorescence intensity of tubulin by Br-Bn-Nos and DOX in single as well as in combination regimen. Tubulin (2.0 μM) was incubated with Br-Bn-Nos (25 μM) and DOX (0.1 μM) alone as well as in combination regimen (25 μM of Br-Bn-Nos and 0.01 μM of DOX) and the emission spectra were collected (310 nm – 400 nm). Both Br-Bn-Nos and DOX in single as well as in combination regimen showed a concentration-dependent quenching of the intrinsic tubulin fluorescence emission intensity indicating the binding of both Br-Bn-Nos and DOX to tubulin. The more reduction in tubulin fluorescence intensity in combination regimen of both Br-Bn-Nos and DOX, compared to their single binding, revealed combination effect with the tubulin. The graph is a representative of three independent experiments.

Figure 11. Enhancement of tubulin-ANS fluorescence by Br-Bn-Nos and DOX in single as well as in combination regimen. Tubulin (2.0 μM) was incubated without (control) or with Br-Bn-Nos (25 μM), DOX (0.1 μM) and in their combination regimen (Br-Bn-Nos 25 μM+DOX 0.01 μM), followed by incubation with ANS (50 μM). The samples were excited at 380 nm and the emission spectra were collected (390 to 500 nm). The increase is more in tubulin-ANS fluorescence in combination regimen of both Br-Bn-Nos and DOX, compared to their single binding, and revealed combination effect with the tubulin. The graph is a representative of three independent experiments.

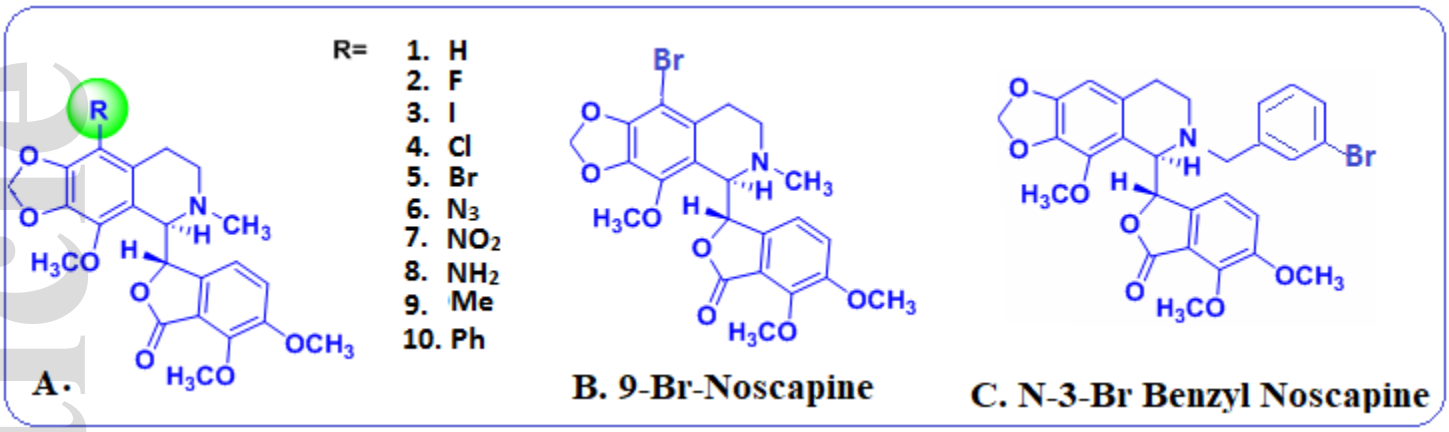

cbdd_13902_f1.tif

cbdd_13902_f2.tif

cbdd_13902_f3.tif

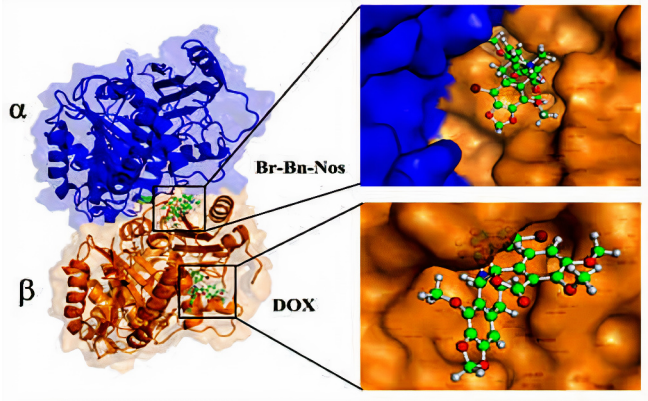

cbdd_13902_f4.jpg

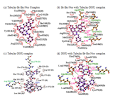

cbdd_13902_f5.tif

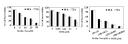

cbdd_13902_f6.tif

cbdd_13902_f7.tif

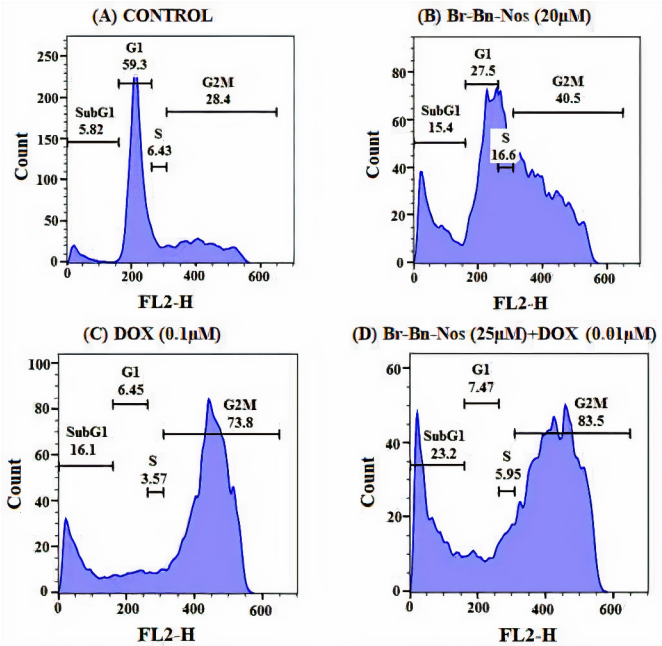

cbdd_13902_f8.jpg

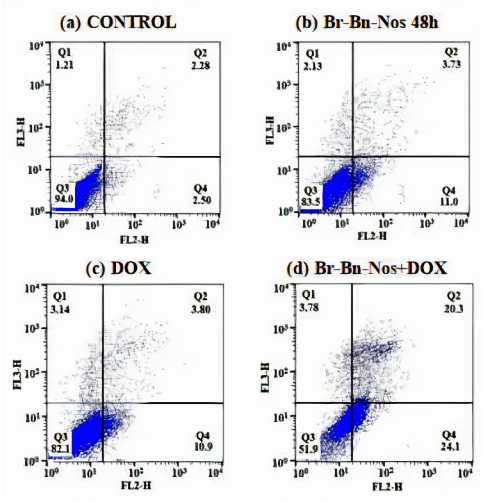

cbdd_13902_f9.jpg

cbdd_13902_f10.jpg

cbdd_13902_f11.jpg